

Phytosome-hyaluronic acid systems for ocular delivery of L-carnosine

Hamdy Abdelkader^{1,2}

Michael R Longman¹

Raid G Alany^{1,3}

Barbara Pierscionek⁴

¹Drug Discovery, Delivery and Patient Care (DDPC) Theme, School of Life Sciences, Pharmacy and Chemistry, Kingston University London, Kingston Upon Thames, London, UK; ²Department of Pharmaceutics, Faculty of Pharmacy, Minia University, Minia, Egypt; ³School of Pharmacy, The University of Auckland, Auckland, New Zealand; ⁴Vision Cognition and Neuroscience Theme, Faculty of Science, Engineering and Computing, Kingston University London, Kingston Upon Thames, London, UK

Abstract: This study reports on L-carnosine phytosomes as an alternative for the prodrug N-acetyl-L-carnosine as a novel delivery system to the lens. L-carnosine was loaded into lipid-based phytosomes and hyaluronic acid (HA)-dispersed phytosomes. L-carnosine-phospholipid complexes (PC) of different molar ratios, 1:1 and 1:2, were prepared by the solvent evaporation method. These complexes were characterized with thermal and spectral analyses. PC were dispersed in either phosphate buffered saline pH 7.4 or HA (0.1% w/v) in phosphate buffered saline to form phytosomes PC1:1, PC1:2, and PC1:2 HA, respectively. These phytosomal formulations were studied for size, zeta potential, morphology, contact angle, spreading coefficient, viscosity, ex vivo transcorneal permeation, and cytotoxicity using primary human corneal cells. L-carnosine-phospholipid formed a complex at a 1:2 molar ratio and phytosomes were in the size range of 380–450 nm, polydispersity index of 0.12–0.2. The viscosity of PC1:2 HA increased by 2.4 to 5-fold compared with HA solution and PC 1:2, respectively; significantly lower surface tension, contact angle, and greater spreading ability for phytosomes were also recorded. Ex vivo transcorneal permeation parameters showed significantly controlled corneal permeation of L-carnosine with the novel carrier systems without any significant impact on primary human corneal cell viability. Ex vivo porcine lenses incubated in high sugar media without and with L-carnosine showed concentration-dependent marked inhibition of lens brunescence indicative of the potential for delaying changes that underlie cataractogenesis that may be linked to diabetic processes.

Keywords: lipid S 75, phytosomes, L-carnosine, cataract, hyaluronate sodium, ocular delivery

Introduction

L-carnosine is a β -alanyl histidine dipeptide and is endogenously present in appreciable amounts in skeletal muscles, the human lens, and in relatively lower concentrations in other human tissues.¹ Its exact physiological function is unknown but, enhancing buffering capacity of the cell recovery from muscle fatigue and cell membrane stabilization are the main identifiable metabolic roles ascribed to this dipeptide.¹ In addition, carnosine is known for its indirect intracellular antioxidant activity that is capable of preventing the accumulation of oxidized products derived from lipid peroxidation of cell membranes. This effect is more likely to be indirect by potentiating the effect of the lipid soluble antioxidant α -tocopherol.¹

Recently, other potential therapeutic benefits of L-carnosine have been highlighted, notably the slowing of ageing processes and the protection from senile cataract formation. L-carnosine has been used in the form of a prodrug (N-acetyl carnosine) to enhance its permeation through the cornea. N-acetyl carnosine in turn is hydrolyzed by esterase in the aqueous humor to release L-carnosine to the lens.^{2,3}

Correspondence: Raid G Alany; Hamdy Abdelkader

Drug Discovery, Delivery and Patient Care (DDPC) Theme, School of Life Sciences, Pharmacy and Chemistry, Kingston University London, Penrhyn Road, Kingston Upon Thames, Surrey KT1 2EE, UK
Tel +44 20 8417 9000; +44 7440 714 585
Email r.alany@kingston.ac.uk;
h.abdelkader@kingston.ac.uk

The use of a prodrug might improve corneal permeation; some studies have shown promising results for such an approach in rabbit and in human eyes.²⁻⁴ However, the process relies on the activity of ocular esterase, which is a protein, and as such might be susceptible to advanced glycation with ageing and/or be expressed in lower levels as an inevitable consequence of ageing.^{5,6} Either way, the ocular bioavailability of the active form might be adversely affected and ultimately might affect the anticataractogenic potency. In this study, the potential of adopting a lipid-based formulation along with a viscosity enhancement approach was explored in an attempt to modulate corneal permeation of the parent form L-carnosine; this is likely to provide an attractive alternative to using the prodrug N-acetyl-L-carnosine.

Phytosomes are innovative lipid carriers; their size is in the submicron range and, as the name suggests, the candidate drugs are phytopharmaceuticals; ie, of plant origin.^{7,8} In a broader sense, the term phytosomes can be used to describe any complex unit that involves a supramolecular association between phospholipid and a guest drug molecule of favorable physicochemical criteria. For example, mitomycin C is an antibiotic anticancer drug derived from bacteria and has been recently formulated as a phytosome complex.⁹ Phytosomes can be considered as lipid–drug compatible supramolecular complexes; once dispersed in aqueous media, they self-assemble into vesicular structures similar to liposomes but with a different guest localization.⁹ In liposomes, water soluble (WS) drug molecules are trapped in the aqueous core or, in the case of multilamellar liposomes, in other aqueous compartments; whereas, phytosome drug molecules are favorably aligned electrostatically and hydrogen-bound with the phospholipid polar head groups (negatively charged phosphate and positively charged ammonium of the choline moiety). The main advantages of phytosomes are their higher drug-to-carrier load compared with liposomes, that they can be easily stored in a solid/lyophilized form ready for reconstitution,⁸ and their smaller size and biocompatibility which renders them more attractive carriers for hydrophilic drug molecules. Unlike liposomes, not all WS drugs can be loaded into phytosomes. The candidate drug should have a certain polarity and adequate functional groups (eg, COOH, OH, NH₂, –NH– or =NH) that can serve as a platform for electrostatic interactions and hydrogen-bonding with phospholipid polar head groups.⁹

Hyaluronic acid (HA), also called hyaluronan and hyaluronate sodium, is a negatively charged hydrophilic polysaccharide that is naturally distributed throughout

connective tissues, epithelia, synovial fluid in the joints and neural tissues as well as in the vitreous of the eye.¹⁰ HA is composed of repeated units of D-glucuronic acid and N-acetyl-D-glucosamine moieties¹⁰ and has gained increasing popularity in drug delivery, medical, and pharmaceutical applications.¹¹ HA hydrogels of concentrations up to 2% w/v have been utilized for their mucoadhesive properties.¹² Gel-cored liposomes or liposomes entrapping a hydrogel polymer such as HA are advanced as an innovative approach in drug delivery, and liposome integrity and stability have been reported to be enhanced in HA gels with more sustained drug release characteristics.¹³ These promising liposomes are hybrids of lipid vesicles and hydrogels and have been found to be versatile and promising.^{13,14}

HA has been used widely in ophthalmology and HA of relatively low concentrations between 0.1% w/v and 0.3% w/v is commercially available for symptomatic relief of dry eye conditions and for promoting healing after cataract and other refractive surgeries.^{15,16} HA can slow tear evaporation, restore precorneal tear film stability at the ocular surface, and relieve discomfort due to dry eye. Dry eye could be an ocular manifestation of certain systemic conditions, and it has been linked to age-related cataractogenesis.¹⁷ This study aimed at investigating L-carnosine as a potential alternative to its prodrug N-acetyl carnosine by adopting a novel lipid-based formulation approach. Specific objectives were the preparation, characterization, and evaluation of phytosomes and phytosome-HA systems to establish their potential as promising ocular carriers of L-carnosine.

Materials and methods

Materials

L-carnosine, cellophane membrane (molecular weight cutoff 12,000–14,000 Da), nitro blue tetrazolium (NBT), and MTT were purchased from Sigma-Aldrich Co. (St Louis, MO, USA). HA was purchased from Acros Organics, (Thermo Fisher Scientific, Waltham, MA, USA). Ammonium molybdate was purchased from Hopkin & Williams Ltd, Chadwell Heath, England. Lipoid s 75 was donated by Lipoid GmbH, Ludwigshafen, Germany. All other chemicals and reagents were of analytical grade and used as received.

Preparation of L-carnosine–phospholipid complex

L-carnosine and lipoid s 75 in molar ratios of 1:1 and 1:2, were separately dissolved in MilliQ (deionized) water (10 mL) and methanol (30 mL) respectively, mixed in a 100 mL round bottom flask and refluxed for 1 hour at 40°C.

The solvent was removed by rotary evaporation in a Buchi rotary evaporator (Buchi, Flawil, Switzerland).⁸ The prepared phospholipid complexes (PC) were transferred into sealed glass vials and stored at ambient conditions ($15^{\circ}\text{C}\pm 5^{\circ}\text{C}$) for further use.

Characterization of the prepared L-carnosine-PC

Differential scanning calorimetry

Samples of L-carnosine powder, Lipoid S 75, PC of 1:1 and 1:2 mol/mol ratios were weighed (typically 5–8 mg) separately in an aluminum pan, covered with an aluminum lid and hermitically sealed using a pan press. The temperature of the pan was gradually increased from 25°C to 300°C at a rate of $10^{\circ}\text{C}/\text{min}$ using a differential scanning calorimeter (Mettler Toledo Differential scanning calorimetry [DSC] 822e0, Greifensee, Switzerland) pre-calibrated with indium. The purging gas was nitrogen at a flow rate of 45 mL/min. Data were collected online using Mettler STARe software version 8.10.

Fourier transform-infrared spectroscopy

The Fourier transform-infrared (FT-IR) spectra for L-carnosine, Lipoid S 75, PC1:1 and PC1:2 were recorded using an FT-IR spectrometer (Thermo Scientific Nicolet is5, Thermo Fisher Scientific). A clean diamond window was used to measure the background spectrum. A sufficient amount (approximately 2–4 mg) of the sample was placed to form a thin film covering the diamond window. The data were acquired and analyzed using Omnic software (Omnic version 8.2, Thermo Fisher Scientific). The FT-IR spectra were recorded at spectral resolution of 2 cm^{-1} with an average of 20 scans.

X-ray diffraction studies

The X-ray diffraction (XRD) analysis of L-carnosine, Lipoid S 75, PC1:1, and PC1:2 was performed using an X-ray diffractometer (Bruker AXS D8 Advance; Bruker Corporation, Billerica, MA, USA). The X-ray diffractograms were scanned at 40 kV tube voltage at room temperature and the scanning diffraction angle (2θ) ranged from 2° to 45° with a step size of 0.1° . The data were collected online using software DIFFRAC plus XRD commander version 2.3 (Bruker Corporation).

Preparation of L-carnosine–phospholipid dispersions

Specified amounts of the prepared solid formulations PC1:1 (500 mg) and PC1:2 (900 mg) equivalent to 1% w/v of

L-carnosine were dispersed in 10 mL of phosphate buffered saline (PBS) warmed to 40°C and vortexed for 5 minutes to form phytosomal dispersions. An additional batch of PC1:2 was dispersed in PBS containing 0.1% w/v HA and labeled PC1:2 HA. Free L-carnosine molecules were separated from those in complex with phytosomal vesicles by extensive dialysis through a cellulose membrane of molecular weight cutoff 1,200–14,000 Da. Samples (2 mL each) of the prepared phytosomes were transferred into a dialysis bag and subjected to extensive dialysis for 2 hours (100 mL of PBS each) at 4°C . The encapsulation efficiency was estimated as described elsewhere.^{18,19}

Characterization of L-carnosine-phospholipid dispersions

Particle size and zeta potential measurements

The particle size, polydispersity index (PDI), and zeta potential of PC1:1, PC1:2, and PC1:2 HA were analyzed (after a suitable dilution of 1:30 with PBS) by dynamic light scattering using a Malvern Zetasizer 3000HSA (Malvern Instruments, Malvern, UK) at 25°C . Zeta potential was measured by laser Doppler electrophoresis using the same instrument under the same conditions. Size values were reported as mean hydrodynamic diameter. All measurements were done in triplicate.

Transmission electron microscopy

Imaging of selected PC formulations was performed using the transmission electron microscope (JEM 1010, JEOL, Tokyo, Japan) with an acceleration voltage of 80 kV. Samples were diluted with PBS (1:30). A drop of the diluted sample was placed on a carbon-coated copper grid and allowed to leave a thin film on the grid before being stained by adding one drop of a solution of 2% w/v ammonium molybdate in ammonium acetate buffer (2%). The stained films were imaged and photographed using JEOL software.

Contact angle, surface tension, spreading coefficient, and viscosity measurements

Contact angle (θ) measurements were performed using a drop shape analyzer (goniometer) (Kruss Drop Shape Analysis, Hamburg, Germany). A Hamilton syringe was filled with each of the tested phytosomal formulations. Approximately 20 μL of each formulation was dropped onto a glass slide at ambient conditions. The image of the drop was captured and measured by Kruss software. The measurements were performed in triplicate and results were presented as mean values \pm standard deviation.

The tendency for spreading can be quantified in terms of the spreading coefficient (S) using Equation 1.²⁰

$$S = \gamma_{L/A} (\cos \theta - 1) \quad (1)$$

where $\gamma_{L/A}$ is the surface tension of the liquid. If θ is larger than 0° , the term $(\cos \theta - 1)$ and the value of S will be negative. The condition for complete or spontaneous wetting is thus a zero value for the contact angle. The surface tension (γ) values of carnosine solution and the prepared phytosomes (PC1:1 and PC1:2) were determined at ambient conditions using an interfacial tensiometer (Kibron, Inc., Helsinki, Finland). Data were collected online using Aqua PI plus software (Kibron, Inc., Helsinki, Finland). All measurements were performed in triplicate.

The viscosity of the prepared drug solution and formulations was studied using a Brookfield viscometer (Brookfield DV-II+Pro; Brookfield AMETEK, Middleboro, MA, USA) equipped with an S62 spindle. The measurements were performed at 25°C .

Ex vivo permeation studies using excised porcine eyes

Enucleated porcine eyes were carefully examined for any corneal damage, such as epithelial scarring, corneal opacity, and corneal vascularization, before the cornea was dissected. The dissection was performed with extreme care to avoid touching the surface of the cornea. A small ring of scleral tissue was left around the cornea. The scleral tissue served as a gasket and the cornea was mounted with endothelium facing the receptor compartment and epithelium facing the donor compartment.

Franz-diffusion cells were used for ex vivo permeation studies, and the temperature was kept at $35^\circ\text{C} \pm 0.5^\circ\text{C}$. The receptor chambers were filled (12 mL) with a PBS (pH 7.4) solution supplemented with 2.4 mM glucose. The medium was constantly stirred using small magnetic bars. A sample (2 mL) of each formulation was transferred into the donor compartment providing surface area of 1.7 cm^2 . Samples (0.4 mL) were withdrawn at predetermined time points for up to 8 hours and replaced with the same volume of the receptor medium without drug. The samples were analyzed using an in-house developed high performance liquid chromatography method. The method was developed and validated according to International Conference on Harmonization guidelines and has been recently published.¹⁹ In brief, the high performance liquid chromatography system (Shimadzu LC-2010AHT, Shimadzu Corporation, Kyoto, Japan) comprised a quaternary pump, an automatic sampler and a UV detector with

data acquisition by Lab solutions software version 5.42 SP5 (Shimadzu Corporation). The chromatographic separation was achieved using a Supelcosil C18 column ($5 \mu\text{m}$; $250 \times 4.6 \text{ mm}$, Supelco Inc, Sigma-Aldrich Co., St Louis, MO, USA) maintained at 40°C . The mobile phase was composed of 0.1% v/v trifluoroacetic acid pH 2.5 (98% v/v) and acetonitrile (2% v/v). The isocratic flow rate was 1.0 mL/min and the injection volume was fixed at $30 \mu\text{L}$. Detection was carried out at a wavelength of 220 nm.

Ex vivo permeation data analysis

The apparent permeability coefficient (P_{app} , cm/s) was calculated using Equation 2.²¹

$$P_{\text{app}} = \frac{\Delta Q}{\Delta t (3600) A C_0} \quad (2)$$

where $\Delta Q/\Delta t$ is the permeability rate of L-carnosine across the excised porcine cornea and it was equal to the gradient of the L-carnosine permeated (Q) versus time (t) curve; C_0 is the initial drug concentration ($\mu\text{g}/\text{cm}^3$); A is the corneal surface area (cm^2). The lag time was determined graphically by extrapolating the steady-state line to the time axis.

Cytotoxicity evaluation of phytosomes (MTT assay)

Primary human corneal epithelial cells (ATCC pcs-700-010) from American Type Culture Collection, (Manassas, VA, USA) were prepared and seeded out at approximately 2×10^4 cells/well into 96-well plates (Nunc, Sigma-Aldrich Co.) in Corneal Epithelial Cell Basal Medium containing the following supplements (LGC standards): apo-transferrin (5 mg/mL), epinephrine (1.0 mM) extract P (0.4%), hydrocortisone hemisuccinate (100 ng/mL), L-glutamine (6 mM), rh insulin (5 mg/mL), and CE growth factor (1 mL, proprietary formulation). Cells were allowed to establish for 48 hours prior to treatment in the 96-well culture plate. Media were subsequently removed and fresh media containing treatments (eight wells used per condition) added. The treatments were as follows: plain carriers of a concentration of 8% equivalent to the amount of lipid in PC1:2 formulation and half carrier concentration (4% w/v); L-carnosine solution of 1% w/v and half the drug solution (0.5% w/v); PC1:2 and half PC1:2 and PC1:2 HA. The medium was used as a negative control and benzalkonium chloride (BKC) at a concentration of 0.01% w/v was used as a positive control. After 24 hours of treatment, the media were removed and the cells washed twice with 37°C sterile PBS. The cells were then incubated with $200 \mu\text{L}$ per well of 0.5 mg/mL MTT solution in 37°C Corneal Epithelial

Cell Basal Medium (LGC standards). After incubation, the MTT solution was carefully removed and the wells washed twice with sterile PBS. Finally, 200 μ L of dimethyl sulfoxide was added to each well to lyse the cells. The cells were gently agitated to mix the samples and analyzed on a TECAN Infinite M200 pro plate reader (Männedorf, Switzerland) at a wavelength of 540 nm. Experiments were performed in triplicate.

Incubation of porcine lenses in high sugar media with and without L-carnosine

Excised porcine eyes were collected fresh from a local abattoir. Each eye was dissected from the posterior segment to extract the whole lens. Lens was rinsed in the medium M199 supplemented with 8% fetal bovine serum and antibiotics (penicillin/streptomycin, 100 units/mL) and then transferred onto a six-well plate (NuncTM Delta Surface, Roskilde, Denmark) containing 10 mL of the medium and incubated for 12 hours at 35°C/5% CO₂.²² Any lens that showed any sign of opacity due to poor dissection was discarded. The incubated lenses were divided into four groups: a negative control (the lenses were incubated in the culture medium without galactose), positive controls (the lenses were incubated in a medium containing 30 mM galactose), and two treated groups containing 30 mM of galactose and 10 mM or 20 mM of L-carnosine and incubated at 35°C/5% CO₂. The media were changed daily for 3 days. Opacity of the lenses was evaluated visually on a grid. Whole lenses were homogenized in a flacon tube with 8 mL of Tris-HCl buffer pH 8.4 containing 0.02% sodium azide. The homogenate was centrifuged at 10,000 rpm for 30 minutes at 4°C. The supernatant was collected to obtain WS fraction of lens crystallins.²³

NBT assay

This assay is based on the reducing properties of the advanced glycation end products or manifesting as conversion of fructosamine to NBT to formazan (purple color) under alkaline conditions.^{24,25} An aliquot of 100 μ L of WS fractions was added to 1 mL of NBT (0.3 M in carbonate buffer pH 10.35). The mixtures were incubated at 37°C for 10 minutes, allowed to cool down to room temperature, and measured spectrophotometrically at 530 nm. Percentage glycated crystallins was estimated using Equation 3:

$$\% \text{ glycated crystallins} = \frac{OD_s - OD_c}{OD_c} * 100 \quad (3)$$

where OD_s is the optical density of the positive control or treated samples and OD_c is the optical density of the negative control.

Statistical analysis

Statistical analysis was performed with Graph Pad Prism 6 (GraphPad Software, Inc., La Jolla, CA, USA), using analysis of variance with a Dunnett post hoc test for confidence intervals of 95% with statistical significance set at $P < 0.05$.

Results and discussion

DSC studies

The DSC studies were carried out to investigate the crystallinity of L-carnosine and the possibility of formation of L-carnosine-phospholipid solid complexes that can be the base for formation of phytosomes after dispersion in the aqueous media. Figure 1 shows the thermal behaviors of L-carnosine, lipoid s 75, PC1:1, and PC1:2. The upper trace shows a sharp and strong endothermic peak at 268°C that is caused by L-carnosine melting. Lipoid S 75 did not show any thermal events in the range of 40°C–300°C as a result of its low melting point. For PC1:1, the appearance of a broad endothermic peak at 250°C could be ascribed to the residual L-carnosine crystallites and appearance of a new peak at 114°C was likely to have been caused by formation of a new complex between the dipeptide drug and the phosphatidylcholine of Lipoid S 75. Complete disappearance of the L-carnosine melting peak and appearance of a new endothermic peak at 114°C indicate the formation of a new complex. The latter thermal event of PC1:2 can be ascribed to potential electrostatic interactions and hydrogen bonding between the dipeptide drug and phosphatidylcholine. Similar results were reported with the phospholipid complex of diosmin. A ratio of diosmin:phospholipid at 1:2 mol/mol showed complete disappearance of diosmin melting peak (291.5°C) and appearance of a new melting peak at 160°C suggestive of a complex formation.⁸

The drug-HA compatibility studies were performed in an attempt to show any possible physiochemical interactions of the polysaccharide carrier HA with the drug. The thermograms of L-carnosine did not show any obvious changes in the melting points (Figure 1); this indicates that there are no physicochemical interactions between L-carnosine and HA that might alter or disrupt L-carnosine PC after dispersion.

FT-IR spectroscopy

FT-IR spectroscopy was employed to further understand the potential interactions between L-carnosine and phosphatidylcholine (the major constituent in Lipoid S 750), as shown in Figure 2. Characteristic IR vibrational peaks in the high-frequency region included stretching vibration at 3,237 cm⁻¹ and 3,049 cm⁻¹ for the amide hydrogen and

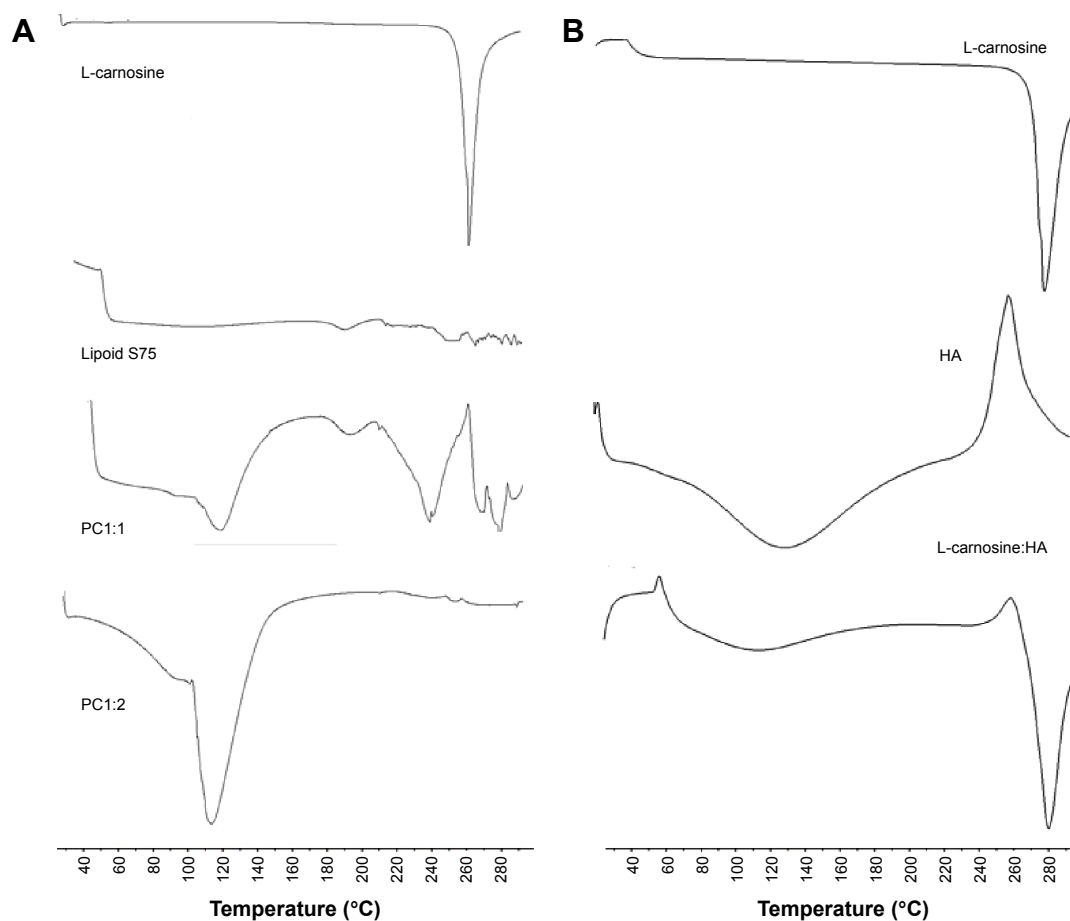


Figure 1 DSC thermograms for L-carnosine, lipid s 75, PC1:1, PC1:2, HA (A), and L-carnosine:HA 1:1 (B).

Abbreviations: DSC, differential scanning calorimetry; PC, phospholipid complexes; HA, hyaluronic acid.

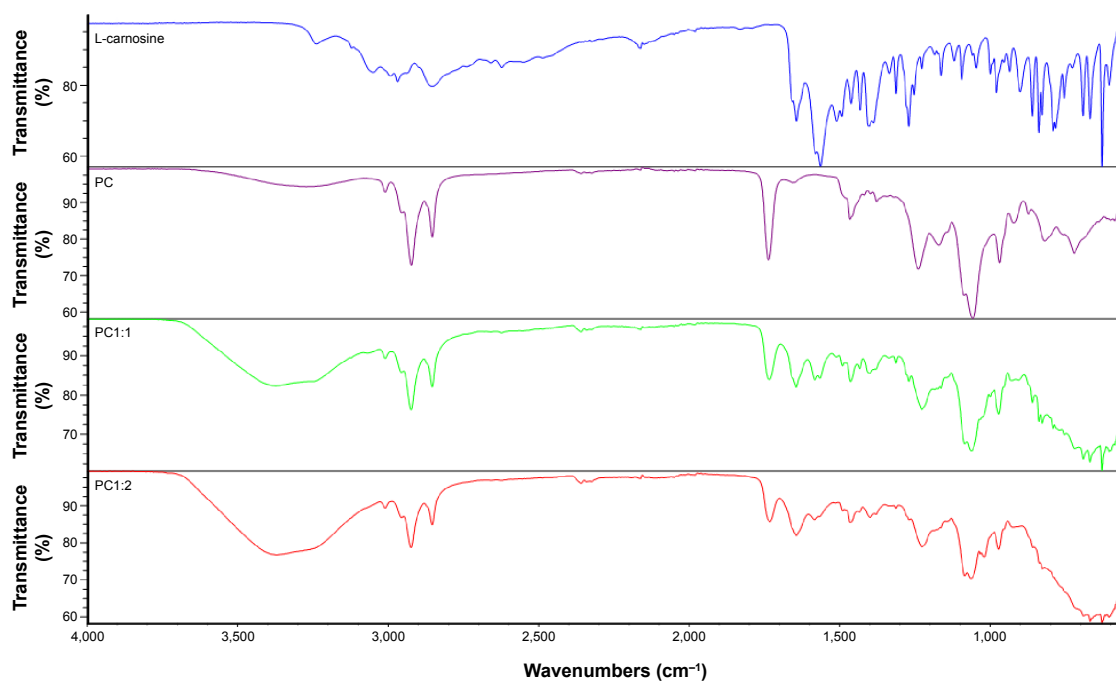


Figure 2 FT-IR spectra for L-carnosine, lipid s 75, and PC1:1 (left trace) and PC1:2 (right trace).

Abbreviations: FT-IR, Fourier transform-infrared; PC, phospholipid complexes.

protonated terminal amine (NH_3^+) of the free L-carnosine.²⁶ Other important peaks were at $2,162\text{ cm}^{-1}$ and $1,643\text{ cm}^{-1}$ due to vibrational bending of imidazole (N-H) and amide group stretching respectively.²⁶

For Lipoid S 75, strong absorption peaks assigned at $2,922\text{ cm}^{-1}$ and $2,852\text{ cm}^{-1}$ were the result of antisymmetric and symmetric stretching of acyl chains (CH_2), respectively. Another strong absorption peak at $1,738$ was caused by ester carbonyl (C=O) group stretching.²⁷ All these characteristic peaks and their characteristic wavenumbers were recorded for PC1:1, indicating no detectable interactions at 1:1 ratio. While these bands were distinctly representative of L-carnosine, their disappearance in the case of PC1:2 could be attributed to the shielding effect of lipid s 75, hydrogen bonding, and formation of L-carnosine phosphatidylcholine complex. Appearance of a broad strong absorption peak at $3,371\text{ cm}^{-1}$ was due to H-bond formation of the amide ($-\text{CONH}-$) with phosphate groups of lipid s 75 and disappearance of the characteristic L-carnosine peak at $2,162\text{ cm}^{-1}$.

XRD studies

Figure 3 shows the XR diffractograms for L-carnosine, lipid s 75, PC1:1, and PC1:2. The L-carnosine showed sharp XRD peaks that are typical of a highly crystalline drug. Lipoid S 75 showed an intense diffraction peak only at $3\ 2\theta$ and the intermolecular spacing was found to be 31.47Å . This can be attributed to an intermolecular space between a stack

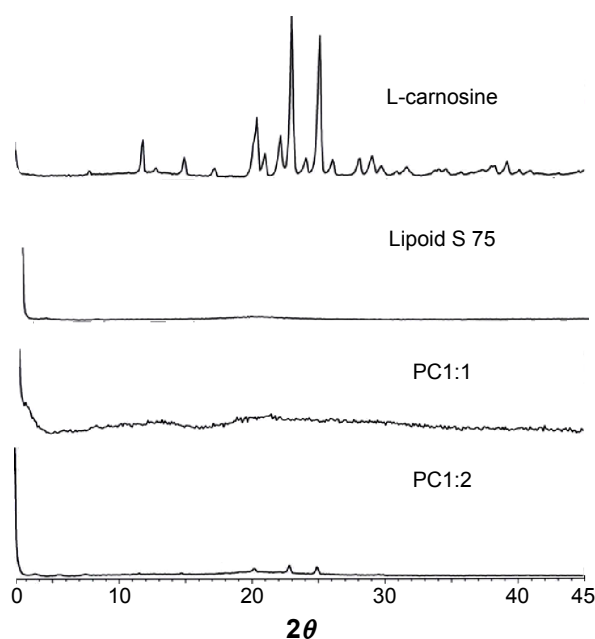


Figure 3 X-ray diffractograms of L-carnosine, Lipoid S 75, and phytosomal complexes (PC1:1 and PC1:2).

Abbreviation: PC, phospholipid complexes.

of hydrocarbon chains in a smectic liquid crystalline state of Lipoid S 75. For PC1:1 and 1:2, the main characteristic peaks of L-carnosine appeared at diffraction angles of 20 , 22.8 , and $25\ 2\theta$. These characteristic peaks were detected at low, broader, and decreasing intensities, which are indicative of residual crystallites of L-carnosine. The DSC results and appearance of a single peak at much lower intensity compared with the pure drug suggest a complex formation at 1:2 molar ratio and the complex melting peak is at a temperature of 112°C .

Size and zeta potential measurements

Table 1 shows that the prepared complexes, when dispersed in aqueous medium (PBS) and in PBS containing HA (0.1% w/v), can self-assemble into phytosomes with a size range of $380\text{--}450\text{ nm}$ and narrow size distributions, as shown from PDI values, and high negative zeta potential values. These dipeptide-PC are negatively charged because of the high electron density generated by the fully ionized phosphate groups of the phospholipids within the neutral pH medium of the PBS.⁹ PC1:1 demonstrated a significantly larger average size (450 nm), compared with PC1:2 (385 nm) and PC1:2 HA (380 nm). This can be attributed to the fact that PC1:1 is an incomplete complex with free L-carnosine molecules and free negatively charged head groups of phospholipids that can self-assemble into phytosomes of a relatively larger hydrodynamic radius, mainly due to electrostatic repulsion. However, PC1:2 is a complete complex and the polar head groups of the phospholipids were partially neutralized and therefore could self-assemble into smaller sized L-carnosine phytosomes. It is worth noting that dispersion of phytosomes in HA had no significant impact on sizes of L-carnosine phytosomes. However, addition of HA reduced the PDI and it may be that increasing the viscosity of the dispersion medium reduced the tendency of vesicles to aggregate. PC1:2 already has a high zeta potential value and is equally well dispersed in either PBS or PBS containing HA (0.1% w/v). Similar results were also reported with the entrapment efficiency (EE%). PC1:2 vesicles showed a marked increase in EE% (85%) compared with that estimated for PC1:1 (55%). This 1.5-fold increase in the EE% for phytosomes PC1:2 can be attributed to the vesicles having sufficient PC molecules to self-assemble into phytosomes, and as a result more L-carnosine molecules become favorably entrapped in the phytosomes rather than in bulk solution. Addition of HA (viscosity enhancing agent) resulted in a slight improvement of EE% (90%) for PC1:2 HA, compared with 85% for PC1:2. A slight increase in the viscosity is likely

Table 1 Size, PDI, entrapment efficiency (EE%), zeta potential, contact angle, surface tension, and spreading coefficient (S) measurements of L-carnosine solution compared with phytosomes

Formulation	Size (nm)	PDI	EE% (w/v)	Zeta potential (mV)	Contact angle (θ°)	Surface tension (mN/m)	S (mN/m)
L-carnosine*	–	–	–	–	50±2.0	76±0.5	–38±1.0
PC1:1	450±26	0.2	55%±3.5%	–48±7.5	38±1.8	42.5±0.8	–9.0±0.5
PC1:2	385±11	0.15	85%±4%	–56±11	42±2.0	43±1.0	–11±0.5
PC1:2 HA	380±15	0.12	90%±6%	–58±9.5	62±2.5	45±2.0	–25±0.7

Note: *L-carnosine solution of 1% w/w was prepared in PBS. The dash indicates that no data was available.

Abbreviations: PDI, polydispersity index; PC, phospholipid complexes; HA, hyaluronic acid; PBS, phosphate buffered saline.

to enhance EE% due to improving L-carnosine complexation with PC molecules.

Transmission electron microscopy

Transmission electron microscopy (TEM) was employed to study the size and the shape of the dispersed phytosomes PC1:2. Figure 4 shows a representative TEM micrograph for PC1:2; the left frame shows the dispersed spheres in a matrix of recrystallized PBS salts, while the right frame is a magnification of the dispersed system showing characteristic spherical structures (PC1:2 phytosomes) with a diameter comparable to that measured using dynamic light scattering.

Contact angle, surface tension, and spreading coefficient measurements

Table 1 shows the surface tension (γ) measurements for the prepared phytosomes compared with L-carnosine aqueous solution in PBS. The γ values measured for the prepared phytosomes were 42.5, 43, and 45 mN/m. These results revealed γ values for the prepared phytosomes that were significantly lower than those for the aqueous solution (76 mN/m) ($P<0.001$). However, there was no significant difference amongst the γ values measured for the prepared phytosomes ($P>0.05$).

It is well established that the lower the surface tension, the easier it is for the formulations to wet the hydrophobic surface of the corneal epithelium.^{28,29} These values for the tested

L-carnosine phytosomes were approximately equal to that of the average surface tension of the tear fluid (43.6±2.7 mN/m) of human eyes.³⁰ This is likely to allow the carriers to mix uniformly with greater miscibility and minimal disturbance to the precorneal tear film, compared with the drug solution in PBS which has a relatively higher surface tension (76 mN/m). The lower the surface tension of the ocular formulation, the less likely it is to disturb the precorneal tear film and induce irritation due to excessive tear evaporation; the negative correlation between surface tension and tear break up time has been previously reported.^{30,31}

Table 1 shows the contact angle (θ) and the spreading coefficient (S) measurements of the prepared formulations compared with the plain vehicle (PBS).

The θ values of all tested phytosomes in PBS (38° and 42°) were significantly lower ($P<0.05$) than those of the aqueous vehicle (50°) and PC1:2 HA (62°). Additionally, the S values of the prepared formulations were up to 1.5 to 4 times greater than those of the aqueous vehicle. These results suggest that spreading of phytosomes on the solid surface is more energetically favored and that the prepared formulations have better wetting properties than does the aqueous vehicle. Hence, the prepared formulations could more promptly and easily wet, spread, and adhere to the hydrophobic surface of the cornea than an aqueous drug solution. The relatively lower spreading ability of PC1:2 HA compared with PC1:2 is likely to be due to the relatively high viscosity of HA

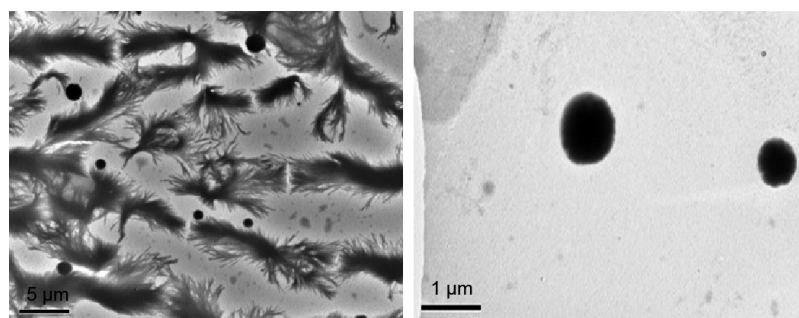


Figure 4 Representative TEM micrograph of PC1:2 phytosomes.

Abbreviations: TEM, transmission electron microscopy; PC, phospholipid complexes.

hydrogel. The greater viscosity of PC1:2 HA compared to PC1:2 means that the former can retain the L-carnosine in contact with ocular surface longer than the latter, which compensates somewhat for the relatively lower spreading ability of PC1:2 HA.

Figure 5 shows the viscosity values of drug solution and the prepared formulations at 25°C. The viscosity values for the prepared phytosomes and HA were significantly higher ($P < 0.01$) than the drug in the aqueous vehicle. The viscosity range was found to be 3 to 12 times higher than that for the aqueous vehicle at 25°C. The highest value for PC1:2 HA was 35 mPa.s, compared to values for HA and PC1:2 of 15 and 7 mPa.s, respectively. This significant increase ($P < 0.01$) could be attributed to the ability of phytosomes to strengthen the network formed by HA caused by interactions of phospholipids with D-glucuronic acid and N-acetyl-D-glucosamine chains. Similar results were reported with liposomes dispersed in HA hydrogels, where the elasticity and viscosity of HA hydrogel were markedly enhanced in the presence of liposome dispersions.¹³

It has been reported that an increase in the viscosity range over 1 to 12.5 mPa.s using methylcellulose as a viscosity imparting agent resulted in a threefold decrease in the precorneal drainage rate. This decrease in the drainage rate increased the concentration of drug in the precorneal tear film.³² In addition, Isopto® and Liquifilm® are widely used commercial viscous vehicles for enhancing the ocular bio-availability of some drugs formulated in simple eye drops. These viscous vehicles consist of 0.5% hydroxypropyl methylcellulose and 1.4% polyvinyl alcohol. The viscosity ranges for these products are 10–30 mPa.s and 4–6 mPa.s, respectively,

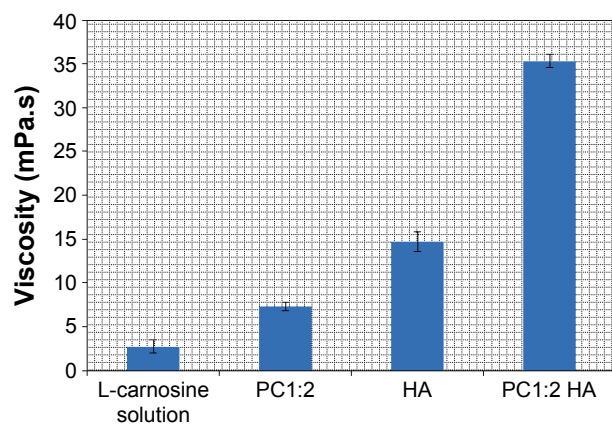


Figure 5 Viscosity values of L-carnosine solution (1% w/v) compared with HA and phytosomes (PC1:2 and PC1:2 HA).

Note: Results are expressed as mean values \pm SD, $n=3$.

Abbreviations: PC, phospholipid complexes; HA, hyaluronic acid; SD, standard deviation.

and both have the convenience of being an eye drop.³³ These findings indicate that the prepared phytosomes have favorable viscosity ranges for prolonged precorneal retention and are indeed in line with currently marketed products.

Ex vivo permeation study

Transcorneal permeation profiles of L-carnosine from drug solution and different phytosomal formulations through excised porcine cornea are shown in Figure 6. Table 2 shows transcorneal permeation parameters of L-carnosine from the investigated formulations. The following transcorneal permeation parameters were calculated: steady-state flux, apparent permeability coefficient (P_{app}), and lag time (t_L) (Table 2). The prepared phytosomes achieved controlled L-carnosine permeation through the corneal tissue compared with L-carnosine solution. The steady-state flux and P_{app} calculated for L-carnosine solution were 2.4 to 5.6 times faster than those for PC1:2 and PC1:2 HA, respectively. While the drug solution showed better permeation rates compared with the prepared PC and PC HA systems on the static receptor compartment of the Franz diffusion model used in this study, there is an ample body of research to suggest that this pattern can be reversed in vivo.^{34–36} L-carnosine took longer time to dissociate from and/or partition through phytosomes bilayer membranes, and further time to diffuse through HA matrix from PC 1:2 and PC 1:2 HA, respectively. Similar results were reported for lipid-based delivery systems, such as liposomes,

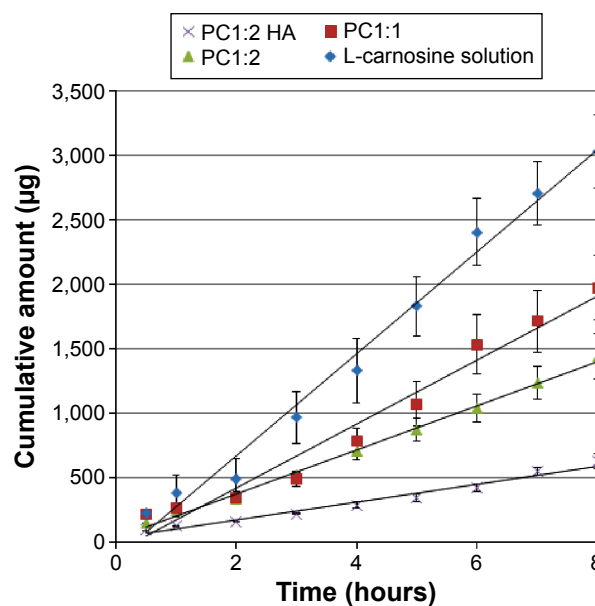


Figure 6 Transcorneal permeation profiles of L-carnosine from drug solution and from different phytosomal formulations.

Note: Results are expressed as mean values \pm SD, $n=3$.

Abbreviations: PC, phospholipid complexes; HA, hyaluronic acid; SD, standard deviation.

Table 2 Steady-state flux, apparent permeability coefficient (P_{app}), lag time, and regression coefficient of L-carnosine

Formulation	Steady-state flux ($\mu\text{g/h}$)	$P_{app} \times 10^{-6}$ (cm/s)	Lag time (min)	Regression coefficient (R^2)
L-carnosine*	390 \pm 32	9.0 \pm 0.2	20 \pm 4.2	0.995
PC1:1	250 \pm 26	7.0 \pm 0.1	15 \pm 3.0	0.987
PC1:2	200 \pm 15	4.5 \pm 0.1	10 \pm 2.8	0.996
PC1:2 HA	70 \pm 4.0	0.8 \pm 0.2	29 \pm 0.5	0.998

Note: *L-carnosine solution of 1% w/w was prepared in PBS.

Abbreviations: PC, phospholipid complexes; min, minutes; HA, hyaluronic acid; PBS, phosphate buffered saline.

niosomes, and solid lipid nanoparticles, using excised rabbit, excised bovine, and bioengineered human corneal samples.^{34–36} The permeation rate and apparent permeability coefficient for acyclovir-encapsulated liposomes and timolol maleate (TM)-loaded solid lipid nanoparticles were more controlled compared with those of the corresponding drug solutions. When these acyclovir liposomes, which demonstrated lower permeability, were applied to rabbit eyes, higher ocular bioavailability for acyclovir was obtained, compared with that for the aqueous drug solution.³⁴ More recently, similar results were also reported with niosomes; the hypotensive effects of topically instilled TM into rabbit eyes were significantly greater with TM niosomes compared with that from TM solution.³⁷

This is attributed to the ability of lipid-based vesicles (liposomes, niosomes, and most likely phytosomes) to provide longer precorneal residence time and less precorneal drug loss than the aqueous solution because of tear dilution and spillage. Furthermore, phytosomes can spread more evenly on the lipophilic corneal membrane as they have better spreading ability and a significantly lower contact angle and favorable viscosity (Table 1 and Figure 5). More interestingly, the ability of L-carnosine to form a complex with PC is more likely to improve the loading capacity of phytosomes as a carrier for the WS cargo (L-carnosine) compared with conventional liposomes. Figure 7 postulates how L-carnosine-PC can self-assemble into phytosomes in

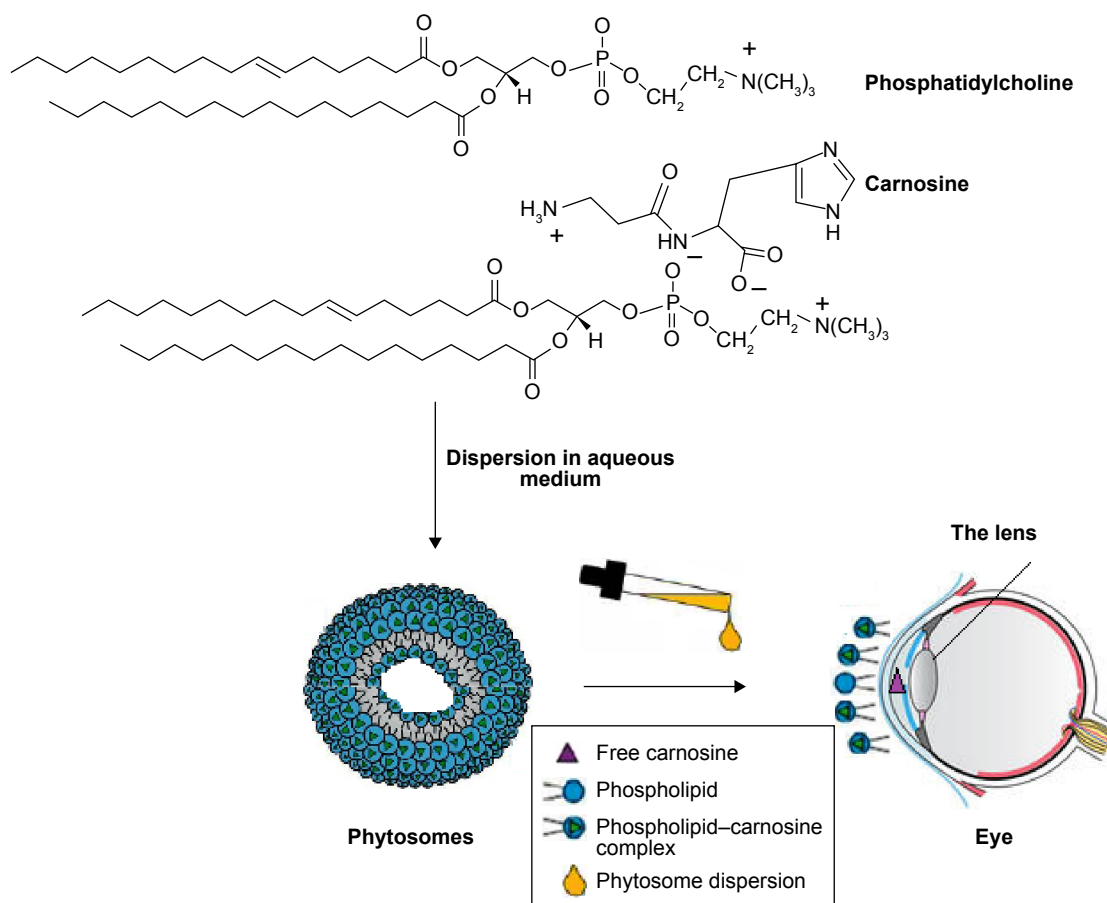
**Figure 7** Graphical representation of self-assembly of L-carnosine phytosomes and drug delivery to the lens.

Table 3 Primary human corneal epithelial cell viability (%) after 24-hour exposure to the test substances employing MTT assay

Formulation	Cell viability (%)	Statistical significance to the medium
Media (negative control)	100	
BKC (positive control)	18±0.63	$P<0.05$
PC alone (8%)	78±15	$P>0.05$
PC alone (4%)	92±24	$P>0.05$
L-carnosine (1%)	76±13.5	$P>0.05$
L-carnosine (0.5%)	85±19.5	$P>0.05$
PCI:2	69±12	$P>0.05$
Half PCI:2	80.5±11	$P>0.05$
PCI:2 HA	77±6	$P>0.05$

Abbreviations: BKC, benzalkonium chloride; PC, phospholipid complexes; HA, hyaluronic acid.

aqueous medium and potentially overcome the outer-coat barrier (cornea) into the anterior chamber and then to the lens.

Cytotoxicity evaluation (MTT assay) of phytosomes to primary human corneal cells

Table 3 shows estimated cell viability after a 24-hour exposure to different treatments. The positive control (BKC) has been shown to be cytotoxic at the duration tested in this study.^{38–40} While there were slight decreases in cell viability after exposure to the different formulations and L-carnosine solution, these were not statistically significant compared to the negative control ($P>0.05$). It is worth noting that BKC (which

for durations comparable to this study is cytotoxic) is used routinely as a preservative in too many commercially available eye drops at a concentration of 0.01% w/v; the duration of exposure of BKC to the eye when applied in eye drops is considerably shorter. These findings indicate that phytosomes in the concentrations and for the durations tested do not demonstrate cytotoxicity in primary human epithelial cells.

Lens incubation in high sugar media

Induction of experimental cataract is an important approach used to gain a better understanding of cataract formation and to help develop potential therapeutic treatments that could delay or reverse cataractogenesis. Galactose was used in this study to induce cataract formation in vitro in excised porcine lenses. On day 3, harvested lenses from negative and positive controls and treated groups were placed on a grid to investigate optical quality. Lenses, incubated in a high galactose medium, showed marked yellowing/browning of lens cortex, compared with control lenses incubated in a medium free of galactose. This characteristic lens “brunescence” is a consequence of glycation and is likely to mimic the processes that underlie diabetic cataract. Lens brunescence was partially inhibited by supplementing the media with 10 mM L-carnosine, those incubated with 20 mM L-carnosine demonstrated lens clarity and lack of brunescence comparable to the negative controls (Figure 8).

The percentage of lens protein glycation recorded in the positive control was at least 30%, whereas treatment with

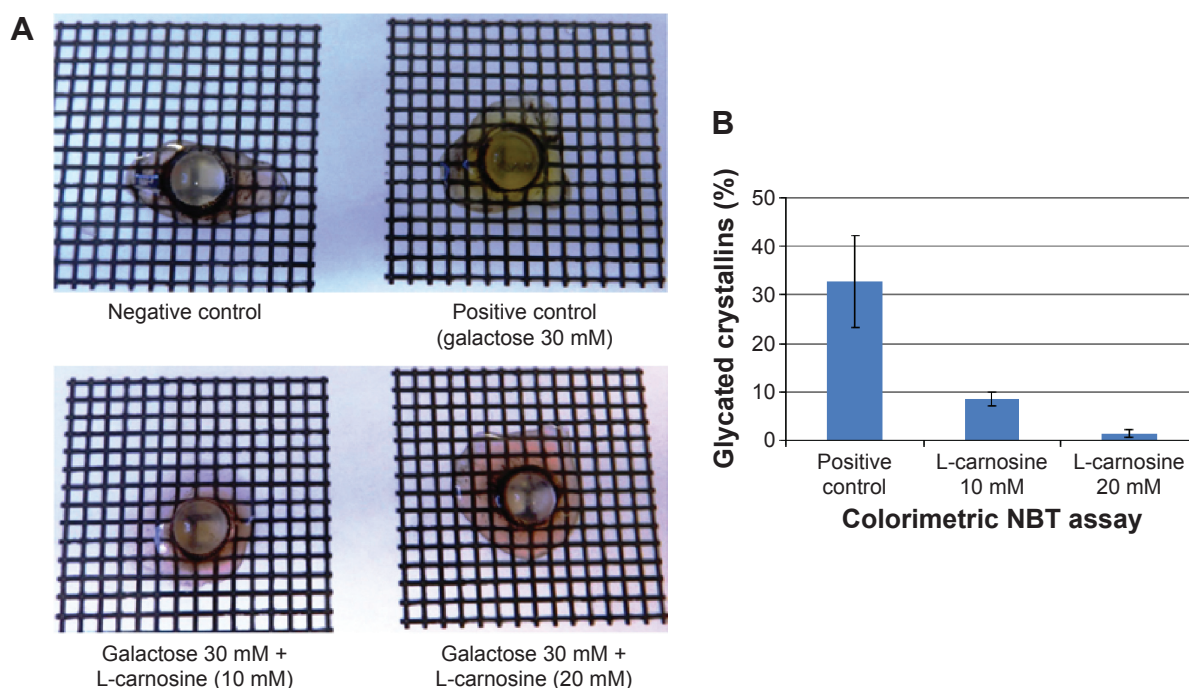


Figure 8 Porcine lenses incubated in negative control medium, in high galactose medium, in high galactose with 10 mM L-carnosine, and high galactose with 20 mM L-carnosine (A); percentage glyated proteins (B).

Abbreviation: NBT, nitro blue tetrazolium.

L-carnosine showed a significant inhibition ($P < 0.05$) in the percentage of glycated proteins (Figure 8).

Conclusion

This study highlighted that formulating L-carnosine utilizing novel lipid-based carriers is a feasible approach. Combining HA hydrogel and lipid-based phytosomes using a simple and scalable preparation method has shown favorable rheological characteristics, spreading ability, sustained drug permeation, and tolerability characteristics for potential ocular delivery of L-carnosine. L-carnosine showed significant inhibition of lens browning as well as formation of advanced glycation end products suggesting that L-carnosine is worthy of further investigation as a promising prophylaxis for diabetic cataract.

Acknowledgments

This work is partially funded by The Cultural Affairs and Missions Sector, Ministry of Higher Education, Cairo, Egypt, in the form of a postdoctoral grant for Dr Abdelkader. The authors acknowledge funding from the Leverhulme Trust and thank Lipoid GmbH, Ludwigshafen, Germany, for the gift of Lipoid S 75.

Disclosure

The authors report no conflicts of interest in this work.

References

- Quinn PJ, Boldyrev AA, Formazuyk VE. Carnosine: its properties, functions and potential therapeutic applications. *Mol Aspects Med*. 1992; 13(5):379–444.
- Babizhayev MA, Burke L, Micans P, Richer SP. N-Acetylcarnosine sustained drug delivery eye drops to control the signs of ageless vision: glare sensitivity, cataract amelioration and quality of vision currently available treatment for the challenging 50,000-patient population. *Clin Interv Aging*. 2009;4:31–50.
- Babizhayev MA, Deyev A, Yermakova VN, et al. Efficacy of N-acetyl-carnosine in the treatment of cataracts. *Drugs R D*. 2002;3(2):87–103.
- Bron AJ, Brown NA, Sparrow JM, Shun-Shin GA. Medical treatment of cataract. *Eye (Lond)*. 1987;1(Pt 5):542–555.
- Kinirons MT, O'Mahony MS. Drug metabolism and ageing. *Br J Clin Pharmacol*. 2004;57(5):540–544.
- Tessier FJ. The Maillard reaction in the human body. The main discoveries and factors that affect glycation. *Pathol Biol (Paris)*. 2010;58(3): 214–219.
- Kidd PM. Bioavailability and activity of phytosome complexes from botanical polyphenols: the silymarin, curcumin, green tea, and grape seed extracts. *Altern Med Rev*. 2009;14(3):226–246.
- Freag MS, Elnaggar YS, Abdallah OY. Lyophilized phytosomal nano-carriers as platforms for enhanced diosmin delivery: optimization and ex vivo permeation. *Int J Nanomedicine*. 2013;8:2385–2397.
- Hou Z, Li Y, Huang Y, et al. Phytosomes loaded with mitomycin C-soybean phosphatidylcholine complex developed for drug delivery. *Mol Pharm*. 2013;10(1):90–101.
- Fraser JR, Laurent TC, Laurent UB. Hyaluronan: its nature, distribution, functions and turnover. *J Intern Med*. 1997;242(1):27–33.
- Ren YJ, Zhou ZY, Cui FZ, Wang Y, Zhao JP, Xu QY. Hyaluronic acid/polylysine hydrogel as a transfer system for transplantation of neural stem cells. *Journal of Bioactive and Compatible Polymers*. 2009;24(1): 56–62.
- Kim JT, Lee DY, Kim YH, Lee IK, Song YS. Effect of pH on swelling property of hyaluronic acid hydrogels for smart drug delivery systems. *Journal of Sensor Science and Technology*. 2012;21(4):256–262.
- El Kechai N, Bochet A, Huang N, Nguyen Y, Ferrary E, Agnely F. Effect of liposomes on rheological and syringeability properties of hyaluronic acid hydrogels intended for local injection of drugs. *Int J Pharm*. 2015;487(1–2):187–196.
- El-Refaie WM, Elnaggar YS, El-Massik MA, Abdallah OY. Novel self-assembled, gel-core hyalurosomes for non-invasive management of osteoarthritis: in-vitro optimization, ex-vivo and in-vivo permeation. *Pharm Res*. 2015;32(9):2901–2911.
- Gomes JA, Amankwah R, Powell-Richards A, Dua HS. Sodium hyaluronate (hyaluronic acid) promotes migration of human corneal epithelial cells in vitro. *Br J Ophthalmol*. 2004;88(6):821–825.
- Shimmura S, Ono M, Shinozaki K, Toda I, Takamura E, Mashima Y. Sodium hyaluronate eyedrops in the treatment of dry eyes. *Br J Ophthalmol*. 1995;79(11):1007–1011.
- Abdelkader H, Alany RG, Pierscionek B. Age-related cataract and drug therapy: opportunities and challenges for topical antioxidant delivery to the lens. *J Pharm Pharmacol*. 2015;67(4):537–550.
- Abdelkader H, Ismail S, Kamal H, Alany RG. Design and evaluation of controlled release niosomes and discomes for naltrexone hydrochloride ocular delivery. *J Pharm Sci*. 2011;100(5):1833–1846.
- Abdelkader H, Swinden J, Pierscionek BK, Alany RG. Analytical and physicochemical characterisation of the senile cataract drug dipeptide β -alanyl-L-histidine (carnosine). *J Pharm Biomed Anal*. 2015;114: 241–246.
- Florence AT, Attwood D. Properties of the solid state. In: Florence AT, Attwood D, editors. *Physicochemical Principles of Pharmacy*. London: McMillan press Ltd.; 1998:5–35.
- Schoenwald RD, Huang HS. Corneal penetration behavior of beta blocking agents I: Physicochemical factors. *J Pharm Sci*. 1983;72(11): 1266–1272.
- Sivak JG, Yoshimura M, Weerheim J, Dovrat A. Effect of hydrogen peroxide, DL-propranolol, and prednisone on bovine lens optical function in culture. *Invest Ophthalmol Vis Sci*. 1990;31(5):954–963.
- Kisic B, Miric D, Zoric L, Ilic A, Dragojevic I. Antioxidant capacity of lenses with age-related cataract. *Oxid Med Cell Longev*. 2012; 2012:467130.
- Loste A, Marca MC. Fructosamine and glycated hemoglobin in the assessment of glycaemic control in dogs. *Vet Res*. 2001;32(1):55–62.
- Oppel K, Kulcsár M, Bárdos L, et al. A new, modern, cost-saving micro/macro method for the determination of serum fructosamine. *Acta Vet Hung*. 2000;48(3):285–291.
- Branham ML, Singh P, Bisetty K, Sabela M, Govender T. Preparation, spectrochemical, and computational analysis of L-carnosine (2-[(3-aminopropanoyl)amino]-3-(1H-imidazol-5-yl)propanoic acid) and its ruthenium (II) coordination complexes in aqueous solution. *Molecules*. 2011;16(12):10269–10291.
- Tamm LK, Tatulian SA. Infrared spectroscopy of proteins and peptides in lipid bilayers. *Q Rev Biophys*. 1997;30(4):365–429.
- Pawar PK, Majumdar DK. Effect of formulation factors on in vitro permeation of moxifloxacin from aqueous drops through excised goat, sheep and buffalo corneas. *AAPS PharmSciTech*. 2006;7(1):E13.
- Rathore MS, Majumdar DK. Effect of formulation factors on in vitro transcorneal permeation of gatifloxacin from aqueous drops. *AAPS PharmSciTech*. 2006;7(3):57.
- Tiffany JM, Winter N, Bliss G. Tear film stability and tear surface tension. *Curr Eye Res*. 1989;8(5):507–515.
- Vicario-de-la-Torre M, Benítez-del-Castillo JM, Vico E, et al. Design and characterization of an ocular topical liposomal preparation to replenish the lipids of the tear film. *Invest Ophthalmol Vis Sci*. 2014; 55(12):7839–7847.

32. Chrai SS, Robinson JR. Ocular evaluation of methylcellulose vehicle in albino rabbits. *J Pharm Sci.* 1974;63(8):1218–1223.
33. Lang JC, Roehrs RE, Rodeheaver DP, Missel PJ, Jani R, Chowhan MA. Design and evaluation of ophthalmic pharmaceutical products. In: Banker GS, Rhodes CT, editors. *Modern Pharmaceutics*. New York, USA: Marcel Dekker; 2002:626–717.
34. Law SL, Huang KJ, Chiang CH. Acyclovir-containing liposomes for potential ocular delivery. Corneal penetration and absorption. *J Control Release.* 2000;63(1–2):135–140.
35. Attama AA, Reichl S, Muller-Goymann CC. Sustained release and permeation of timolol from surface-modified solid lipid nanoparticles through bioengineered human cornea. *Curr Eye Res.* 2009;34(8):698–705.
36. Abdelkader H. *Design and Characterisation of Niosomes for Ocular Delivery of Naltrexone Hydrochloride*. PhD thesis. Auckland: The University of Auckland; 2011.
37. Abdelkader H, Farhgaly U, Moharram H. Effects of surfactant type and cholesterol level on niosomes physical properties and in vivo ocular performance using timolol maleate as a model drug. *Journal of Pharmaceutical Investigation.* 2014;44(5):329–337.
38. Ayaki M, Iwasawa A, Inoue Y. Toxicity of antiglaucoma drugs with and without benzalkonium chloride to cultured human corneal endothelial cells. *Clin Ophthalmol.* 2010;4:1217–1222.
39. Eleftheriadis H, Cheong M, Sandeman S, et al. Corneal toxicity secondary to inadvertent use of benzalkonium chloride preserved viscoelastic material in cataract surgery. *Br J Ophthalmol.* 2002;86(3):299–305.
40. Mencucci R, Pellegrini-Giampietro DE, Paladini I, Favuzza E, Menchini U, Scartabelli T. Azithromycin: assessment of intrinsic cytotoxic effects on corneal epithelial cell cultures. *Clin Ophthalmol.* 2013;7:965–971.

International Journal of Nanomedicine

Publish your work in this journal

The International Journal of Nanomedicine is an international, peer-reviewed journal focusing on the application of nanotechnology in diagnostics, therapeutics, and drug delivery systems throughout the biomedical field. This journal is indexed on PubMed Central, MedLine, CAS, SciSearch®, Current Contents®/Clinical Medicine,

Submit your manuscript here: <http://www.dovepress.com/international-journal-of-nanomedicine-journal>

Dovepress

Journal Citation Reports/Science Edition, EMBase, Scopus and the Elsevier Bibliographic databases. The manuscript management system is completely online and includes a very quick and fair peer-review system, which is all easy to use. Visit <http://www.dovepress.com/testimonials.php> to read real quotes from published authors.